STATIONARY EFFLUX INTO A VACUUM BY A DUAL-TEMPERATURE FULLY IONIZED PLASMA

I. I. Litvinov

UDC 533.9+537.56

It is shown that the macroscopic process of plasma discharge from an expanding nozzle is determined, when the thermal conductivity of electrons and heat transfer between the components are taken into account, by a unique dimensionless parameter: the adiabaticity parameter characterizing the transition from adiabatic flow of a dense plasma to the flow of comparatively rarefied plasma when the free path length of the particles is commensurate with the characteristic dimension of the nozzle. A numerical method is used to find the distribution of gas-dynamic and electrical parameters of the plasma stream, and the relationship between the generalized output parameters. It is shown that the energy associated with the ions at infinity, in the latter case, can be tens of times greater than the energy in adiabatic efflux, because of the high thermal conductivity with respect to electrons, but unrealistically large expansion of the nozzle is needed in order to attain it. "Singular" flow patterns occurring when stationary discharge of plasma at infinity is calculated are also discussed.

Theoretical and experimental investigation of the outflow of ionized gas into a vacuum has been the subject of a large number of literature contributions. These contributions discuss the flow of rarefied plasma [1-7] when the mean free path length λ is commensurate with or even less than the characteristic dimension of the source L, and also high-density plasma [8-15] such that $\lambda \ll L$. In the latter case, close attention has been given to the breakdown of ionization equilibrium, temperature equilibrium, or other modes of equilibrium in response to a decline in the initial density of a plasma and its effect on the gas-dynamic parameters of the stream.

In addition to the factors mentioned, the thermal conductivity of an electron gas begins to play a tangible role as the density decreases, which leads to inadiabatic flow regimes. But this effect was not discussed in the papers referred to. Moreover, results published in [12] are asserted by the authors of [12] to be valid even in the case $\lambda \lesssim L$, and the thermal flux of the electrons q_e, which plays a particularly conspicuous role in this case, dropped out of the system of equations altogether.

The purpose of this paper is to report an investigation of the effect of the thermal conductivity of electrons in plasma flow through a nozzle in "pure form," discussing an idealized case of discharge of a fully ionized dual-temperature plasma over a broad range of initial densities. These results are then compared to the conventional adiabatic solution.

1. Qualitative analysis of plasma flow through a nozzle. Below, we make use of a system of equations for a fully ionized dual-temperature plasma [16]. In the one-dimensional stationary case, the continuity equation is

$$NVS = I \tag{1.1}$$

where $N=N_e=N_i$ is the density, $V=V_e=V_i$ is the velocity of the plasma, S is the channel cross section, and I is the flowrate of the particles.

Moscow. Translated from Zhurnal Prikladnoi Mekhaniki i Tekhnicheskoi Fiziki, No. 6, pp. 10-20, November-December, 1971. Original article submitted June 14, 1971.

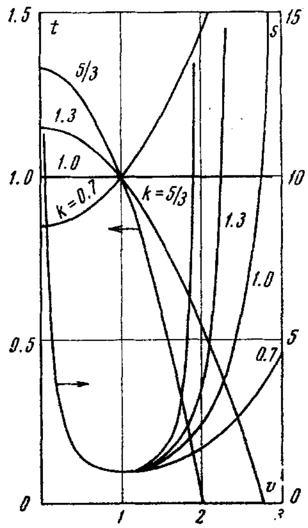

Fig. 1

In place of two separation equations of motion for the electrons and ions, it is convenient to resort to the equation of electron equilibrium

$$0 = -dP_e / dX - eNE + R_T \tag{1.2}$$

and the equation of motion for the plasma as a whole

$$MNVdV / dX = -d(P_e + P_i) / dX \tag{1.3}$$

In Eqs. (1.2), (1.3), $R_T = -0.71\, NdT_e/dX$ is the thermal driving force. In addition, here we neglect the inertia of the electrons ($m/M \ll 1$) and the viscosity.

Of the two energy equations, we make use of the heat equation for the ions

$$\frac{3}{2} NV \frac{dT_i}{dX} + \frac{P_i}{S} \frac{d}{dX}(SV) = Q_\Delta, \quad Q_\Delta = \frac{3m}{M} \frac{N}{\tau_e}(T_e - T_i) \tag{1.4}$$

and the total equation of energy transfer

$$SNV \left[\frac{MV^2}{2} + \frac{5}{2}(T_e + T_i)\right] + Sq_e = H = \text{const} \tag{1.5}$$

where H is the power of the plasma stream.

The equation deals with the heat flux

$$q_e = -\varkappa_e dT_e / dX \qquad (\varkappa_e = 3.16\, NT_e\tau_e / m)$$

while the ion heat flux q_i is neglected in Eq. (1.5).

The role played by the electron thermal conductivity can be estimated with ease from the ratio of the heat flux q_e to the convective heat flux

$$\zeta = \frac{q_e}{NVT_e} \sim \sqrt{\frac{M}{m}} \frac{\lambda_e}{L} \tag{1.6}$$

This makes it evident that the scale of the thermal conductivity effect is the large length [17] $L_0 = \lambda_e\sqrt{M/m}$. When $L \approx L_0$, the heat flux is of convective order. When $L \approx \lambda_e$, the heat flux q_e is overwhelmingly large, and $\zeta \approx \sqrt{M/m} \gg 1$. Note that, when $L \approx \lambda_e$, these results are valid only in order of magnitude, but that their accuracy increases markedly [18] even when L/λ_e is of the order of several units, so that we can arbitrarily take $L \gtrsim \lambda_e$ for the boundary of the range of macroscopic description in the discussion below. The remaining discarded terms in Eqs. (1.2)-(1.5) are substantial on the lengths $\approx \lambda_e$, and can be safely neglected when $L \gg \lambda_e$.

It is clear from Eqs. (1.5) and (1.6) that $\varkappa_e$ is almost independent of N, so that the relative role played by q_e declines with increasing flowrate I, and the flow tends toward an adiabatic regime with the temperature $T = T_e + T_i = 2T_e$ and adiabatic exponent $5/3$. The flow parameters are interrelated by algebraic relationships [10, 19, 20].

When the electron thermal conductivity is brought into the picture, these parameters are also dependent upon the behavior of the process, and the power H in (1.5), in contrast to the parameters N, T_e, T_i, V, is actually, because of the indeterminacy of dT_e/dX in the inlet cross section, an unknown self-adjusting quantity dependent upon the "inlet" parameters mentioned, and on the shape of the channel. A correct solution of this problem presents the principal difficulty encountered in the overall problem.

We seek to clarify, qualitatively, the condition of transition through the speed of sound in the case of this plasma flow pattern accompanied by heating of the plasma. A convenient model for this type of process [17, 19] is the polytropic law

$$P / \rho^k = \text{const}, \qquad \text{or} \qquad T / N^{k-1} = \text{const} \tag{1.7}$$

where k is the polytropic exponent. This approximation makes it possible to arrive, in the usual way via the Bernoulli equation, at the algebraic equation

$$1 - \left(\frac{N}{N_0}\right)^{k-1} = \frac{k-1}{k} \frac{MV_0^2}{2T_0} \left[\left(\frac{V}{V_0}\right)^2 - 1\right] \qquad (k \neq 1) \tag{1.8}$$

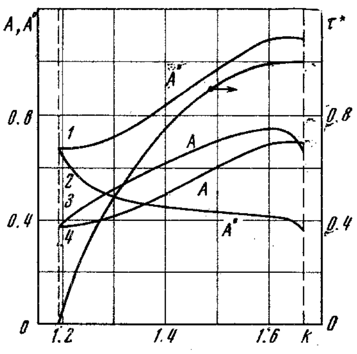

Fig. 2

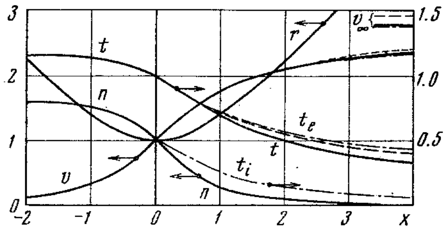

Fig. 3

in which the zero subscript corresponds to variables taken in the initial cross section for the integration. The ratio $MV_0^2/2T_0$ in (1.8) remains undetermined for the time being. By later normalizing all of the variables in Eqs. (1.1), (1.7), (1.8) to their values in this cross section (small letters replacing capital letters), and requiring that this cross section coincide with the critical cross section, for which necessarily $ds/dv = 0$ when $s = 1$, we find the relationship between energy and temperature in the critical cross section so important for the subsequent discussion:

$$\frac{MV_*^2}{2T_*} = \frac{k}{2} \tag{1.9}$$

After that, all the flow parameters can be expressed with ease in terms of the velocity

$$t = \frac{k+1}{2} - \frac{k-1}{2} v^2, \qquad n = t^{(k-1)^{-1}}, \qquad s = n^{-1} v^{-1} \tag{1.10}$$

These dependences are plotted in Fig. 1 for different k values. Clearly, when $k > 1$ the velocity maximum is attained at infinity as $t_\infty \to 0$, so that $v_\infty^2 = (k+1)/(k-1)$. Hence we obtain the usual $v_\infty = 2$ for the adiabatic exponent. When $k \le 1$, the velocity increases without bound over the length of the channel. Consequently, supplying heat to the supersonic part of the nozzle when there is appropriate expansion of the nozzle brings about an increase in the rate of discharge through the nozzle.

We realize from Eq. (1.9) and Fig. 1 that the velocity of the plasma stream passes through a "polytropic" speed of sound $a_* = \sqrt{kP_*/\rho_*}$, where now $P_* = P_e^* + P_i^*$, in the nozzle critical cross section (nozzle throat section). This result is in agreement with the conclusions drawn for an ordinary gas [20]. The dependence of the dimensionless velocity on the cross section in the subsonic part, for different k, is almost identical, so that here it suffices to consider the solution in the supersonic part. This solution is joined below to the polytropic solution in the throat section. Naturally, this solution will be at variance with the polytropic solution when this distance is sufficiently great. But this approximation is highly useful over a broad region [17, 21]. The exact solution also enables us to find the dependence of the effective index k on other parameters characterizing the plasma flow pattern as a whole.

2. System of equations for calculations, and its special features. In order to reduce the system to a form suitable for the Runge-Kutta numerical method, we take as the unknowns the variables T_e, T_i, and the ion energy W. The equations for T_e and T_i are derived from Eqs. (1.5) and (1.4). The equation for W is derived from the momentum equation (1.3) with the relations $-N'/N = S'/S + W'/2W$ from (1.1) taken into account, while the derivative $T' = T_e' + T_i'$ in the right-hand member of the equation is expressed in terms of the equations for T_e and T_i. Here and in what follows, the prime denotes derivatives taken with respect to X.

As we learn from Eqs. (1.4) and (1.5), these equations contain their own characteristic scales within them so that the solution as a whole is dependent upon the nozzle contour. We take as such the normalized cross section in the form of a rounded-off cone:

$$s(x) = 1 + x^2, \qquad x = X / X_* \tag{2.1}$$

The essential features of the solution that are due to the indeterminacy of the power H in Eq. (1.5) are dealt with most simply at the outset, using the example of flow such that $T_i \equiv 0$; the case $T_i \not\equiv 0$ will be discussed later.

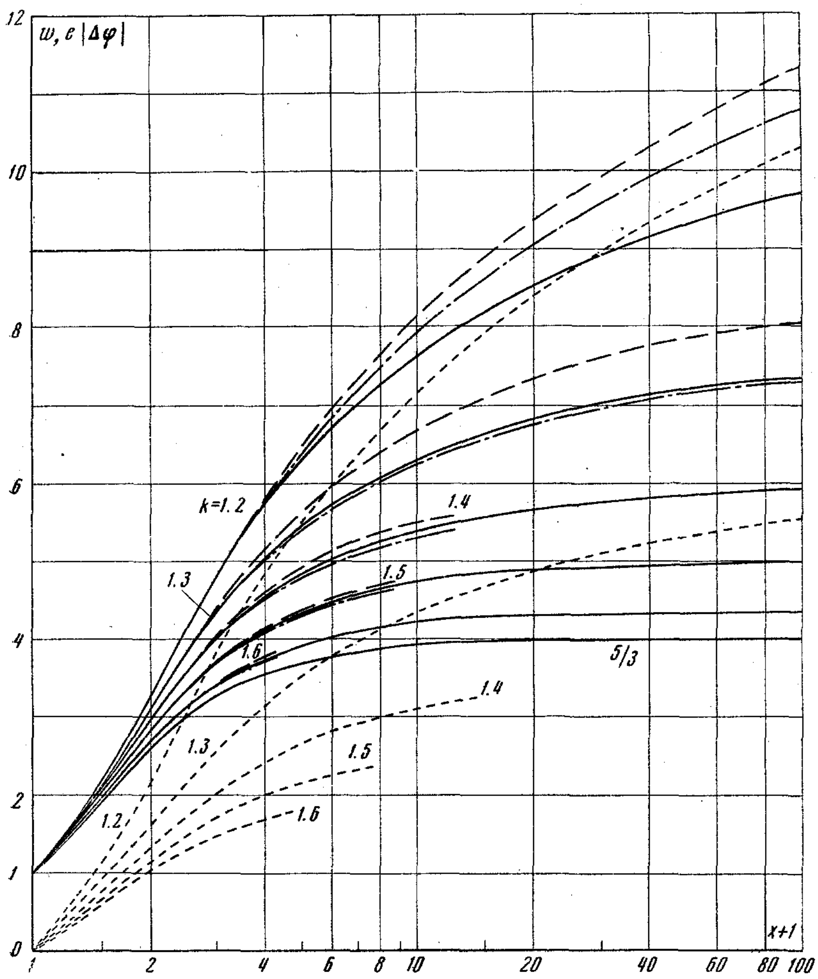

Fig. 4

<u>Flow such that $T_i \equiv 0$.</u> Equation (1.5), in which $T \equiv T_e$, is more conveniently spelled out, because of the indeterminacy of H, in terms of the parameters in the throat (critical) section:

$$\frac{S\varkappa_e}{I} T_e' - \frac{S_*\varkappa_e^*}{I} T_{e*}' = W - W_* + \frac{5}{2}(T_e - T_e^*) \tag{2.2}$$

Later, dividing Eq. (2.2) by T_e^* and then normalizing all of the remaining quantities by their values at $X = 0$ (and the coordinate X by X_*) we find, with Eq. (1.9) taken into account,

$$t_e' = \frac{1}{s t_e^{3/2}} \left\{ t_{e*}' + \frac{\beta}{2}\left[k(w-1) - 5(1-t_e)\right]\right\} \tag{2.3}$$

where $t_e^{5/2} = \varkappa_e/\varkappa_e^*$, and $\beta = IX_*/S_*\varkappa_e^*$ is the dimensionless parameter of the flow pattern.

Similarly, we have the equation for the dimensionless energy

$$\frac{w'}{2}\left(k - \frac{t_e}{w}\right) = t_e \frac{s'}{s} - t_e' \tag{2.4}$$

The dimensionless temperature gradient t_{e*}' appearing in Eq. (2.3) is found from the polytropic solution of Eq. (1.10). By expressing n and w in terms of t in the equation $n^2 w = s^{-2}$, and substituting the series $t = 1 + \tau_1 x + \ldots$, we find, from the equation of the coefficients attached to x^2,

$$\tau_1 = -\frac{\sqrt{2}(k-1)}{\sqrt{k+1}} = t_{e*}' \tag{2.5}$$

Similarly, by using Eq. (2.5), we get $w_*' = \varepsilon_1 = 2\sqrt{2}/\sqrt{k+1}$.

TABLE 1

Gas	$\overset{\circ}{\beta}_{min}\cdot 10^3$	k_{min}	$W^{\infty}_{max}/\overset{\circ}{W}_{\infty}$
H	23.3	1.208	6.5
H_2	16.5	1.203	8.85
He	11.6	1.199	12.1
Li	8.85	1.197	16.2
N_2	4.41	1.1935	31.5
Ar	3.70	1.1930	38.3
Fe	3.12	1.1926	45.0
Zs	2.02	1.1918	68.3
Hg	1.65	1.1916	84.0

And, finally, the flow parameter β, after substitution for the case $T_i \equiv 0$, acquires the form

$$\beta = \frac{1}{3.16}\frac{mv_e{}^*V_*}{T_e{}^*}\frac{X_*}{\lambda_e{}^*} = \frac{2\sqrt{2}}{3.16}\sqrt{\frac{k}{\pi}}\sqrt{\frac{m}{M}}\frac{X_*}{\lambda_e{}^*} \tag{2.6}$$

where $\nu_e{}^* = (8T_e^*/\pi m)^{1/2}$ is the random thermal velocity of the electrons.

The most essential quantity in Eq. (2.6) is the parameter

$$\beta^\circ = \sqrt{\frac{m}{M}}\frac{X_*}{\lambda_e{}^*} \tag{2.7}$$

defined as the ratio of the characteristic dimension X_* of the nozzle to the scale effect of thermal conductivity L_0. Clearly, in this case this is the only generalized control parameter dependent upon the input parameters and on the nozzle geometry. This parameter must also uniquely determine the effective exponent k. In the limit as $\beta^\circ \to \infty$, the flow regime must tend to the adiabatic, and when β° decreases, to the isothermal. Taking the above remarks into account, we can quite naturally term β° the adiabaticity parameter. In practice, however, it is more convenient to specify the value of k beforehand, and to then find β and β°.

In the case of small x values, the expression within the square brackets in Eq. (2.3) becomes

$$^1/_2\,\beta\,[k(w-1) - 5(1-t_e)] \approx {}^3/_4\,\beta\varepsilon_1({}^5/_3 - k)x$$

We readily note, then, on the basis of (2.3), that if the value of β is less than required for a specified $k < {}^5/_3$, then the expression enclosed within the braces in Eq. (2.3) will decrease in absolute value with increasing x insufficiently rapidly, and then t_e will plunge steeply to zero because of the factor $t_e{}^{5/2}$ in the denominator. Similarly, if β is large, then a change of sign to positive will occur within the braces starting with a certain value of x, i.e., t_e will begin to grow. These phenomena have been arbitrarily denoted as the T- and T'-crises.

Clearly, in order to arrive at a solution satisfying the required conditions at infinity $T_e \to 0$, $T_e' \to 0$, iterative adjustment of the parameter $\beta_j(k)$ is called for. This procedure is equivalent to the above-mentioned adjustment of the power in the inlet cross section. Actually, the inlet gradient T'_{e*}, and in this substitution $\beta^\circ(k)$, is an eigenvalue of the nonlinear boundary problem.

In order to determine the first-order approximation $\beta_1(k)$, we consider the behavior of the solution in the neighborhood of $x = 0$. Substituting the series into Eqs. (2.3) and (2.4) for that purpose, we find, for the zero degree,

$$\tau_1{}^e = \tau_1, \qquad \varepsilon_1 = -2\tau_1/(k-1)$$

i.e., the same as for the polytrope. The subsequent coefficients in the expansion of τ_j and ε_j are then expressed in terms of τ_1, ε_1, and β. Recalling further that $|\tau_2|$ is finite and very small, in fact tending to zero in the limit as $k \to 1$, for the polytrope as $k \to {}^5/_3$, we put $\tau_2 \equiv 0$ in the solution in order to determine $\beta_1(k)$.

Hence,

$$\beta_1 = \frac{5\sqrt{2}}{3\sqrt{k+1}}\frac{(k-1)^2}{{}^5/_3 - k} \tag{2.8}$$

This expression satisfies the required dependence $k(\beta^\circ)$ qualitatively.

Adjustment of $\beta_j(k)$ was carried out automatically by dividing the interval $\Delta\beta_j$ between two adjacent β_j corresponding to the T-crisis and T'-crisis in half. As β_j is refined in the calculations, the coordinates of the crises become shifted to higher x values.

Flow such that $T_i \neq 0$. By analogy with Eq. (2.3), we now have

$$t_e' = \frac{1}{st_e^{5/2}}\left\{t_{e*}' + \frac{\beta}{2}\left[k(w-1) - 5\left(1 - \frac{t_e + t_i}{1+\tau_*}\right)\right]\right\} \tag{2.9}$$

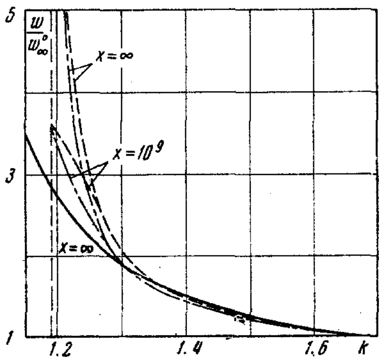

Fig. 5

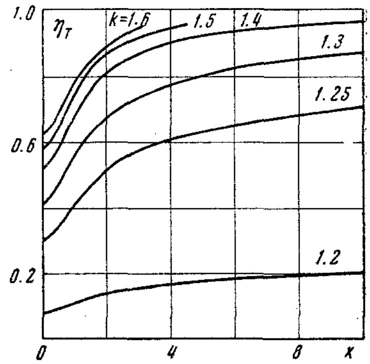

Fig. 6

Now multiplying the equations for W and T_i by the ratio X_*/T_e, we obtain in dimensionless form

$$\frac{w'}{2}\left[k(1+\tau_*)-\frac{1}{w}\left(t_e+\frac{5}{3}t_i\right)\right]=\frac{s'}{s}\left(t_e'+\frac{5}{3}t_i\right)-t_e'-\frac{2}{3}\frac{Q_\Delta SX_*}{IT_e^*} \tag{2.10}$$

$$t_i'=-\frac{2}{3}t_i\left(\frac{s'}{s}+\frac{w'}{2w}\right)+\frac{2}{3}\frac{Q_\Delta SX_*}{IT_e^*} \tag{2.11}$$

In contrast to the general rule, the temperature T_i in Eqs. (2.9)-(2.11) was normalized by T_e^*, with $t_i^*=\tau_*$. Moreover, the adjustment parameter β in Eq. (2.9), in the general case $\tau_*\neq 0$, becomes

$$\beta=(1+\tau_*)IX_*\,/\,S_*\varkappa_e^*$$

In order to reduce the last terms in Eqs. (2.10) and (2.11), denoted as $B_\Delta=B^*b_\Delta$, while recalling Eqs. (1.1) and (1.9), we find

$$b_\Delta=\frac{t_e-t_i}{swt_e^{3/2}}$$

$$B^*=\frac{2m}{M}\frac{\nu_e^*}{V_*}\frac{X_*}{\lambda_e^*}=\frac{4\sqrt{2}}{\sqrt{\pi k}}\frac{\beta^\circ}{\sqrt{1+\tau_*}}$$

Consequently, heat transfer between the components is determined by the same parameter β° as the heat conduction effect.

When β_j is adjusted, the parameters β_j° and B_j^* can be found from the equations

$$\beta_j^\circ=1.58\sqrt{\frac{\pi}{2k}}\frac{\beta_j}{(1+\tau_*)^{3/2}},\qquad B_j^*=\frac{6.32}{k}\frac{\beta_j}{(1+\tau_*)^2} \tag{2.12}$$

In order to determine the dependence $\tau(k)$, we recall that the temperature T_i in a high-density stream ($k\to 5/3$) must tend to T_e ($\tau_*\to 1$) in the case of intense heat transfer ($Q_\Delta\approx N^2$). As k decreases, the ions do not have time to heat up, so that $\tau_*\to 0$. Substituting the series into Eqs. (2.9) and (2.11) once again, and setting the coefficients attached to $x^{(0)}$ equal, we arrive at the formulas

$$\tau_1^e=\tau_1^e,\quad \tau_1^i=-{}^1/_3\tau_*\varepsilon_1+B^*(1-\tau_*),\quad \varepsilon_1=-2\tau_1/(k-1) \tag{2.13}$$

Clearly, the values of τ_1^e and τ_1^i, where τ_1 is now the dimensionless initial gradient of the total temperature

$$\tau_1=(\tau_1^e+\tau_1^i)/(1+\tau_*)$$

must be assigned in order to join the solution to the polytropic solution.

Here τ_1^e and τ_1^i remain arbitrary for the time being. But it is readily realized, from (2.13), that $\tau_1^i\to-\tau_*\varepsilon_1/3$, where $-\varepsilon_1/3$ tends to the adiabatic gradient $\tau_1=-1/\sqrt{3}$, in the limit as $k\to 5/3$. Consequently, if we entertain the natural assumption that τ_1^i is proportional to τ_* and τ_1 for all k ($\tau_1^i=\tau_*\tau_i$), then we again obtain $\tau_1^e=\tau_1$, and we arrive at the equation

$$\frac{\tau_*(1+\tau_*)^2}{1-\tau_*}=\frac{6.32}{\sqrt{2}}\frac{\sqrt{k+1}}{k}\frac{\beta_j}{5/3-k} \tag{2.14}$$

for τ_* from Eqs. (2.13), with Eqs. (2.12) taken into account.

This equation, cubic in τ_*, is readily solved by the Cardan method.

Consequently, the system (2.9)-(2.11), with Eqs. (2.12) and (2.14) taken into cognizance, is entirely ready for computations and for iterative adjustment of β_j, and of the parameters $\tau_*{}^j$, β_j°, B_j^*. We can again take Eq. (2.8) as the first approximation for β_1.

Clearly, the interrelation accepted here, $\tau_1^i = \tau_* \tau_1$, is not the only possible one.

3. Numerical results and discussion. In the adjustment of $\beta_j(k)$, it was found that there is no T-crisis in evidence as k decreases, starting with a certain value of k_*. The explanation of this phenomenon is as follows. Near the threshold (as $k \to k_*$) $\beta \to 0$, so that, by putting $\beta \equiv 0$ and discarding the expression within brackets in Eqs. (2.3) and (2.9), we arrive at the solution

$$t_e = (1 - 7/2 \,|\tau_1|\, \mathrm{arc\,tg}\, x)^{2/7}$$

In the case $|\tau_1| < 4/7\pi$, this solution falls short of attaining zero in the limit as $x \to \infty$. Hence, for the limiting k we have the equation

$$(k-1)/\sqrt{k+1} = 2\sqrt{2}/7\pi$$

whose solution is $k_* = 1.19035$.

The variable k_* depends on the contour r(x) of the nozzle. As the nozzle divergence decreases compared to (2.1), $k_* \to 1$.

As we found when adjusting β and β°, their dependences on k are well described by formulas of the type $A(k-k_*)/(5/3-k)$, where A(k) are multiplicative factors of the order of unity, as plotted in Fig. 2. The curves 1 and 4 refer to the $T_i \equiv 0$ case, and curves 2, 3 refer to the $T_i \not\equiv 0$ case. The dependence $\tau_*(k)$ is also plotted. The dashed vertical lines delimit the range of variation of k from $k_* = 1.19035$ to $k = 5/3$.

Figure 3 shows the typical calculated distribution of gas-dynamic variables for $k = 1.3$ and the contours r(x) according to (2.1). The polytropic solution is handled in similar fashion. Here and in what follows, the curves are plotted as a continuous curve for the polytrope, a broken curve for the case $T_i \equiv 0$, and a dot-dash curve for the case $T_i \not\equiv 0$, in the comparison of the three cases. Clearly, the overall behavior of the solution is very close to the polytropic variation. The difference in the behavior of the temperatures becomes more conspicuous as t_i declines more rapidly than t_e with increasing x, but the total temperature t is also close to the polytropic. As $k \to k_*$, the discrepancy between the exact solution and the polytropic solution widens. It is also evident that the heat transfer effect is of no substantial importance in this case.

In the limit as $k \to 5/3$, the accuracy of the adjustment of β_j (all the way to the ninth significant digit) proves inadequate, because of the large values of β°, to advance the solution appreciably further in the x-direction.

The ion energy distribution for different k values, and the distribution of the potential difference in the stream ($T_i \not\equiv 0$) normalized by W_*, is shown in Fig. 4 (the potential distribution is indicated by the broken curve). The equation for the potential difference $e|\Delta\varphi|$ is derived from Eq. (1.2)

$$e\,|\Delta\varphi|' = \frac{2}{k(1+\tau_*)}\left[t_e\left(\frac{s'}{s} + \frac{w'}{2w}\right) - 1.71\, t_e'\right]$$

Figure 4, and analysis of Eqs. (1.2), (1.3), support an interesting conclusion on the role played by the thermal driving force R_T. Since R_T is an internal force, it has no effect, on the whole, on acceleration of the plasma (see Eq. (1.3)), but does have a substantial effect on another internal force, the electric force, and on the relationship between the potential drop $e|\Delta\varphi|$ and the ion energy w. For example, in the limit as $k \to k_*$, when $T_i \approx 0$, the force eNE is greater than $-dP_e/dX$ by the amount R_T, so that the potential difference can be greater than the ion energy. In the limit as $k \to 5/3$, when the contribution made by the force $-dP_i/dX$ is large, $e|\Delta\varphi|$ is less than w, but a completely determined finite pressure drop materializes in the stream in the case of adiabatic flow ($k = 5/3$).

One important characteristic of the plasma flow regime is the ion energy at infinity. Its value can be found from Eq. (1.5):

$$w_\infty = \frac{H}{IW_*} = 1 + \frac{5}{k} + \frac{2}{k}\,\frac{|\tau_1{}^e|}{\beta} \tag{3.1}$$

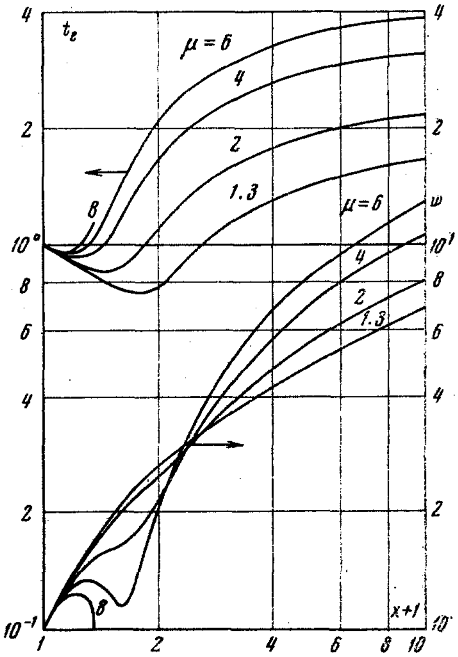

Fig. 7

The last term appearing in Eq. (3.1) defines the contribution made by the thermal conductivity of the electrons. In the limit as $\beta \to \infty$ (adiabat), the role played by q_e is negligible, and then we obtain the usual value $w_\infty = v_\infty^2 = 4$.

In a formal sense, the ion energy at infinity, in the limit as $k \to k_*$, can be as large as we wish, but some essential physical restrictions make themselves felt in this context. The first such restriction is the requirement that the conditions of macroscopic description be met. Then, assuming $\lambda_e^* \lessapprox X_*$ in the throat (critical) section, we can compile a table of limiting values for the several gases in question.

This restriction placed on w_∞ corresponds physically to the fact that the heat flux of electrons q_e^* cannot exceed its own natural upper limit, that of the random heat flux

$$q_e^\circ = 2T_e^* N_* v_e^* / 4 \tag{3.2}$$

In the latter case, we find

$$w_{\max}^\infty = 1 + \frac{5}{k} + \sqrt{\frac{2}{\pi k}} \sqrt{\frac{M}{m}}$$

This is roughly $^4/_3$ times greater than the tabular values.

It must also be recalled that the condition $\lambda_e^* < X_*$ does not consistently eventuate in the condition $\lambda_e < X$ streamwise, in the case of flow of a stream with heating. Actually, when we recall that $\lambda_e = \lambda_e^* t_e^2/n$, we have $\lambda_e = \lambda_e^* n^{2k-3}$ for the polytrope. Similarly, we find $X \approx X_* w^{-0.25} n^{-0.5}$ from the continuity equation, and here $w^{-0.25} \approx 1$. Then the condition $\lambda_e < X$ in the stream goes over into the inequality $n^{2k-2.5} < X_*/\lambda_e^*$; $k > 1.25$ is required to meet that condition in the limit as $n_\infty \to 0$. When $k < 1.25$, starting with a certain value of x, the initial condition $X/\lambda_e^* \gg 1$ no longer holds, and the kinetic solution becomes mandatory later on. It is interesting that, in this case, the parameters β_j, and consequently the stream power H as well, are known with sufficient accuracy, so that the only problem in the kinetic solution is to refine the spatial behavior of the averaged parameters and of the particle distribution functions.

The second condition for validating the macroscopic equations is the condition for the small Debye radius $\delta \ll X$. It can be shown with ease that this condition, which converts to the inequality $n^{0.5(k-1)} \ll X_*/\delta_*$ in the case of a polytrope, is fulfilled all the way to $k = 1$ in the limit as $n_\infty \to 0$. Consequently, the thermal energy of the electrons becomes converted completely, thanks to the electric field E, into the kinetic energy of the ions at infinity, despite the breakdown of the condition $\lambda_e < X$ in the stream.

Let us now compare the ion energy to the energy in adiabatic flow. Limiting ion energies at infinity are plotted for different k in Fig. 5, and theoretically predicted values for sufficiently large x (all the way up to $x = 10^9$) are also plotted. Their values are referred to the adiabatic energy at infinity w_∞°. According to Fig. 5 and Table 1, in the limit as $k \to k^*$ the ion energy at infinity can become tens of times greater than the adiabatic energy. But even when $x = 10^9$ the theoretically predicted energy is not more than 3.7 times greater than the adiabatic energy. This amounts to roughly $W \approx 9T_e^*$. At realistic values $x \approx 10^1$ to 10^2, the ion energy ≈ 5 to $7T_e^*$, which corresponds more or less to the potential of an isolated body in a plasma [5]. This ion energy has been noted on more than one occasion in experiments [5-7, 15]. Taking the above into account, we note that the flow of rarefied plasma such that $\lambda_e^* \approx X_*$ is actually characterized by very low efficiency $\eta_T = F^2/2MIH$, where $F(X) = S(P + MIV)$, since inadmissibly great expansion of the nozzle is required in order to attain $\eta_T \approx 1$ (see Fig. 6). This loss of efficiency is due to the heavy heat losses beyond the accelerator cutoff (this heat is used up in "heating" infinity). A similar conclusion retains its validity for plasma accelerators of other types, in which there is direct thermal contact between the discharge region and infinity.

Note that this loss mechanism is not manifested to its full under laboratory conditions, since the channel length is actually limited by the wall, and the electrons trapped by the charged wall layer carry to the wall a power $H_e = I \cdot 2T_e$, i.e., energy losses for each electron amount to not more than $2T_e$ in contrast to $\approx T_e\sqrt{M/m}$ in the case of outflow to infinity at $\lambda_e^* \approx X_*$. And, in effect, in the presence of wall we require, in place of the conditions applying to T_e at infinity, the boundary condition at the wall, in order to adjust the solution; and this boundary condition can be derived with ease by analogy with the derivation of the diffusional stream of particles [18], by making use of the above-mentioned random heat flux (3.2):

$$T_e = -f\lambda_e \, dT_e / dX \qquad (X = X_w) \tag{3.3}$$

where f is a kinetic coefficient of the order of unity. Constraint (3.3) determines the possibility of successful laboratory simulation of the flow of plasma to infinity. In particular, in this case of rarefied plasma, the two flow regimes must diverge markedly because of the heat flux differences.

It is worth remarking, however, that all inferences as to the state at infinity were drawn for the stationary mode. In the case of the $\lambda_e^* \approx X_*$ flow pattern, when processes taking place over very long channel lengths are essential, the actual flow regime is in effect nonstationary, and the problem calls for closer scrutiny.

The behavior of the solution in "trans-crisis" regimes was also clarified in the course of the computations. It was found that when $\beta < \beta_\infty$ (T-crisis), t_e plunges steeply to zero with a slow increase in w, as previously. The alternative case $\beta > \beta_\infty$ (T'-crisis) was more interesting (see Fig. 7; case $T_i \neq 0$, k = 1.5). In response to a slight rise

$$\mu = \beta / \beta_\infty \gtrsim 1$$

t_e declines at first, then increases and levels off at a constant value. The energy due to the increase in t_e (and also in t_i) increases more rapidly than at $\mu = 1$. This solution corresponds formally to the presence of a heat source upstream. When $\mu = 4$ to 8, the temperatures rise so rapidly that flow becomes blocked. This phenomenon is reminiscent of the heat crisis familiar in aerodynamics [19].

In conclusion, the author thanks I. K. Fetisov for helpful discussion.

LITERATURE CITED

1. A. A. Plyutto, "Acceleration of positive ions in an expanding vacuum spark plasma," Zh. Éksp. Teor. Fiz., 39, No. 6, 1589 (1960).
2. A. A. Plyutto, V. N. Ryzhkov, and A. T. Kapin, "High-velocity streams of vacuum arc plasma," Zh. Éksp. Teor. Fiz., 47, No. 2, 494 (1964).
3. F. Salz, R. G. Meyerand, E. C. Lary, and A. P. Walch, "Electrostatic potential gradients in a Penning discharge," Phys. Rev. Letts., 6, No. 10, 523 (1961).
4. D. J. Rose and R. J. Esterling, "Calculation of distributions in one-dimensional plasma sheaths," J. Appl. Phys., 33, No. 11, 3317 (1962).
5. M. D. Gabovich, Plasma Ion Sources [in Russian], Naukova Dumka, Kiev (1964).
6. M. D. Gabovich, L. I. Romanyuk, and V. V. Ustalov, "Discharge of plasma from a Penning discharge with an incandescent filament into a field-free vacuum region," Zh. Tekh. Fiz., 39, No. 2, 291 (1969).
7. S. A. Andersen, V. O. Jensen, P. Nielsen, and N. D'Angelo, "Continuous supersonic plasma wind tunnel," Phys. Fluids, 12, No. 3, 557 (1969).
8. H. Beckmann and A. J. Chapman, "Thrust from partly ionized monatomic gases," ARS Journal, 32, No. 9, 1369 (1962).
9. M. D. Gabovich, L. L. Pasechnik, and E. A. Lozovaya, "Escape of plasma with high concentration of charged particles into a vacuum," Zh. Tekh. Fiz., 31, No. 9, 1049 (1961).
10. V. M. Sarychev, "One-dimensional motion of a thermally non-equilibrium plasma," Zh. Prikl. Mekhan. i Tekh. Fiz., No. 3, 15 (1962).
11. N. M. Kuznetsov and Yu. P. Raizer, "Electron recombination in plasma expanding into void," Zh. Prikl. Mekhan. i Tekh. Fiz., No. 4, 10 (1965).
12. Y. S. Chou and L. Talbot, "Source-flow expansion of a partially ionized gas into a vacuum," AIAA J., 5, No. 12, 2166 (1967).
13. G. A. Luk'yanov, "Stationary supersonic source of nonequilibrium plasma, Zh. Prikl. Mekhan. i Tekh. Fiz., No. 6, 13 (1968).
14. E. P. Baulin and G. A. Odintsova, "Some aspects of discharge of a plasma of mixtures into a vacuum," in: Generators of Low-Temperature Plasma [in Russian], Énergiya, Moscow (1969).
15. N. V. Afanas'ev, S. N. Kapel'yan, L. P. Filippov, and V. A. Morozov, "Velocities of plasma jets," Zh. Prikl. Spektroskopii, 11, No. 4, 629 (1969).

16. S. I. Braginskii, "Transport phenomena in plasma," in: Reviews of Plasma Physics, Vol. 1, Consultants Bureau (1965).
17. Ya. B. Zel'dovich and Yu. P. Raizer, Physics of Shock Waves and High-Temperature Gas-Dynamic Phenomena [in Russian], Nauka, Moscow (1966).
18. I. I. Litvinov, "Distribution of diffusing particles near an absorbing wall," Zh. Prikl. Mekhan. i Tekh. Fiz., No. 2, 21 (1971).
19. G. N. Abramovich, Applied Gas Dynamics [in Russian], Nauka, Moscow (1969).
20. L. A. Vulis, Thermodynamics of Gas Streams [in Russian], Gosénergoizdat, Moscow (1950).
21. G. A. Dombrovskii, A Method for Approximating the Adiabatic Curve in the Theory of Two-Dimensional Gas Flows [in Russian], Nauka, Moscow (1964).